ResearchGate

See discussions, stats, and author profiles for this publication at: https://www.researchgate.net/publication/7940611

# Directed Self-Assembly of Ge Nanostructures on Very High Index, Highly Anisotropic Si( hkl ) Surfaces

**ARTICLE** *in* NANO LETTERS · MARCH 2005

Impact Factor: 13.59 · DOI: 10.1021/nl048340w · Source: PubMed

CITATIONS
9

READS
24

**6 AUTHORS**, INCLUDING:

Kenji Ohmori
University of Tsukuba
**96** PUBLICATIONS **521** CITATIONS
SEE PROFILE

Ivan Petrov
University of Illinois, Urbana-Champaign
**296** PUBLICATIONS **8,477** CITATIONS
SEE PROFILE

Available from: Ivan Petrov
Retrieved on: 16 January 2016

NANO LETTERS

2005
Vol. 5, No. 2
369−372

# Directed Self-Assembly of Ge Nanostructures on Very High Index, Highly Anisotropic Si(*hkl*) Surfaces

**Kenji Ohmori,* Y. L. Foo,† Sukwon Hong,‡ J. G. Wen, J. E. Greene, and I. Petrov**

*Frederick-Seitz Materials Research Laboratory and Department of Materials Science, University of Illinois, 104 South Goodwin Avenue, Urbana, Illinois 61801*

*Received October 8, 2004; Revised Manuscript Received December 16, 2004*

**ABSTRACT**

**Families of very high-index planes, such as those which bifurcate spontaneously to form a hill-and-valley structure composed of opposing facets, provide natural templates for the directed growth of position-controlled self-organized nanostructures with shapes determined by the facet width ratio *R*. For example, deposition of a few ML of Ge on Si(173 100 373), corresponding to *R*(113/517) = 1.7, results in a field of 40-nm-wide Ge nanowires along [72 187 $\bar{8}$4] with a uniform period of 60 nm.**

The controlled fabrication of nanostructures and surface nanopatterns is a crucial step underlying all fields of nanotechnology. For example, nanoscale architectures on Si surfaces are presently of intense interest due to their compatibility with conventional microelectronic device processing, and hence, their potential for future generations of novel electronic devices. Current strategies to achieve uniform nanostructural arrays include both top-down and bottom-up approaches. In the former case, nanostructure fabrication is generally accomplished through conventional optical lithography techniques in which feature sizes are limited by the radiation wavelength,[1] while bottom-up methodologies have been utilized primarily in self-assembly techniques such as film growth in the strain-induced Stranski−Krastanov (SK) mode. A major bottleneck in both tactics, however, is the lack of control in one or more of the following: size, shape, position, and/or areal density distributions.

Ge growth on Si(001) has been studied extensively as a model SK system due to a combination of the relatively large lattice constant mismatch, 4.2%, as well as compatibility of Ge with Si device processing. A variety of Ge nanostructures including pyramids (huts), domes, and elongated islands are obtained as a function of temperature, growth rate, and film thickness.[2−4] Some progress in controlling the density, size, and spatial uniformity of these structures has been achieved using stacked multilayer growth,[5] ion implantation,[6] and lithographically-assisted deposition.[7] Since the SK growth mode is driven by strain and Si is elastically asymmetric, the shape of deposited Ge nanostructures also depends strongly on substrate orientation.[8] Until now, the primary substrate orientations used have been (001), (113), (110), and (111) due to their stable surface reconstructions.[9]

We have chosen to take a different route and have developed a novel and completely general method for rapidly evaluating all possible substrate orientations, within a given crystal structure, for self-organized nanostructure growth. We use computer-controlled focused ion beam (FIB) etching to fabricate concave circular cones and square pyramids with varying depths. In the case of Si(001) substrates, by systematically changing both the tilt angle $\theta$ of the sidewalls with respect to the (001) plane as well as the in-plane azimuthal direction $\varphi$ with respect to the [$\bar{1}$10] direction, we show that very-high-index Si(*hkl*) planes provide natural templates for the directed growth of uniformly spaced self-organized nanostructures with shapes ranging from isotropic domes to triangles to teardrops to one-dimensional wires under the same deposition conditions. Based upon initial experimental results, we use a surface structural model for the formation of families of nanoscale grooves in order to predict precise $\theta$ and $\varphi$ values for the substrate growth planes required for shape-, size-, and position-controlled self-assembly of as-deposited nanostructures. For example, regular fields of 40-nm-wide, several-$\mu$m-long Ge nanowires with a highly uniform period of 60 nm are grown on Si(173 100 373), corresponding to $\theta = 28.2°$ with $\varphi = 75°$ with respect to the initial Si(001) substrate surface, along the [72 187 $\bar{8}$4] direction. The Si(173 100 373) surface has

* Corresponding author. E-mail: ohmori@mrl.uiuc.edu.
† Present address: Institute of Materials Research and Engineering (IMRE), 3 Research Link, S117602, Singapore.
‡ Present address: School of Materials Science and Engineering, Seoul National University, San 56-1, Shilim-dong, Kwanak-ku, Seoul 151-744, Korea.

10.1021/nl048340w CCC: $30.25 © 2005 American Chemical Society
**Published on Web 01/12/2005**

a hill-and-valley structure which consists of alternating (113) and (517) facets with a (113)/(517) width ratio $R = 1.7$.

The Si(001) substrates used in these experiments have a miscut angle of 0.3° at 2.2° from the [100] direction. The samples are first oxidized at 1000 °C to form a 200-nm-thick $SiO_2$ cap layer in order to avoid excess deformation and penetration of $Ga^+$ ions, typically 30 keV and 3 nA, during FIB sample preparation. After processing, the oxide layer is removed and a protective oxide layer formed using a UV/ozone process.[10] The samples are then introduced into a multichamber gas-source molecular beam epitaxy system (details in refs 11 and 12), where they are degassed at 650 °C and then flashed at 1100 °C to remove the oxide. Si buffer layers, 50-nm-thick, are grown at 800 °C from $Si_2H_6$, after which 7 ML of Ge is deposited at 600 °C from $Ge_2H_6$ (see ref 12 for deposition procedures). Surface morphologies are examined by tapping-mode atomic force microscopy (AFM), while Ge/Si interfaces are analyzed using high-resolution cross-sectional transmission electron microscopy (XTEM) and scanning TEM (STEM).

Figure 1a is an AFM image of one quadrant of a concave truncated circular-cone structure with a depth of 2.3 $\mu$m, fabricated in Si(001), on which 7 ML of Ge has been deposited. The image, 9.0 × 9.0 $\mu m^2$, is high-pass filtered to highlight fine structures on the inclined surface. The image scan direction, for this and all AFM images shown here, is along [$\bar{1}$10] projected onto the (001) plane. Outside the cone structure (i.e., on the Si(001) surface), the Ge islands are dome shaped with a density of 30.9 $\mu m^{-2}$, as expected from previous results.[13] Note that the islands decorate the circular-cone rim where local deviations from (001) provide surface steps that are favorable sites for island nucleation.[14] Figure 1b is a line profile along the azimuthal direction $\varphi = 0$ (i.e., along [$\bar{1}$10]) of the cone in Figure 1a showing both the (negative) feature height $h$ below the rim and the tilt angle $\theta$ as a function of position. The spikes in the $\theta$ vs position curve are due to Ge islands.

The sample in Figure 1 contains a sidewall region approximately 2.5 $\mu$m wide with a constant tilt angle $\theta$ of 28.2±1.5°. A wide variety of island shapes and densities are formed on this conically curved surface as a function of azimuthal position $\varphi$ within the etched crater. For example, a magnified view of the region highlighted by the white square in Figure 1a is presented in 1c, where we broadly classify the Ge nanostructures as (1) domes which are elongated along $\varphi = n90°$ with $n = 0, 1, 2, 3$ (see upper left, Figure 1c), (2) curved nanowires extending approximately 2 $\mu$m long, located near $\varphi \simeq (n90 \pm 15)°$ with $n = 0, 1, 2, 3$ (see middle region: $69° \leq \varphi \leq 83°$), and (3) arc-shaped facetted regions terminated with arrowheads located near $\varphi = (n45 \pm 10)°$ with $n = 1, 3, 5, 7$ (lower right). An extensive library of Ge nanostructure shapes, distributions, and densities has been obtained by systematically varying the dimensions of FIB-produced conical structures etched in the Si(001) substrate (i.e., by varying the orientations of the exposed Si planes).

Here we focus on isolating a high-order Si plane which allows the self-organized growth of straight Ge nanowires

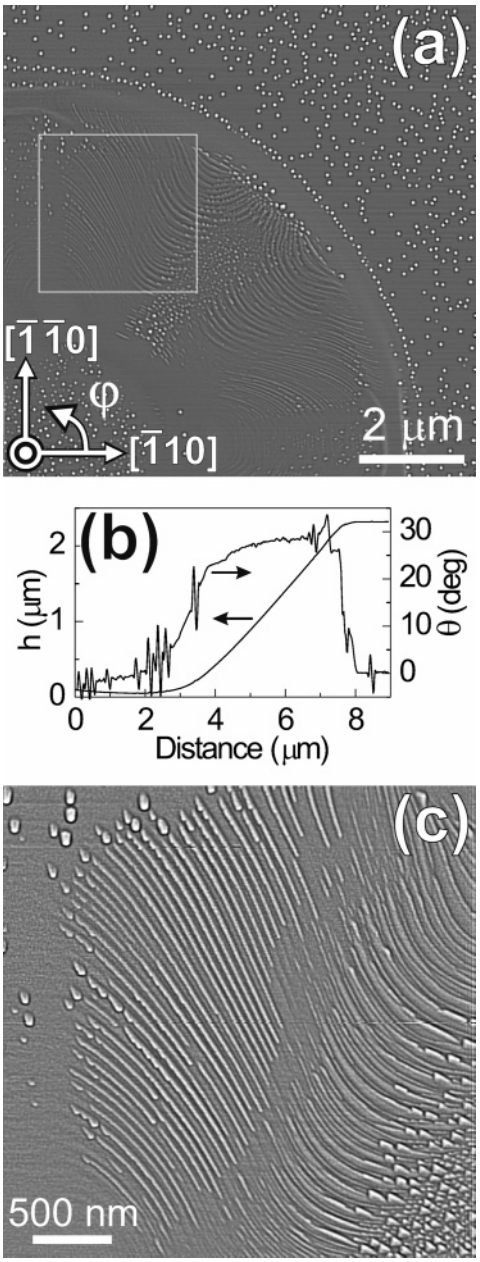


**Figure 1.** Examples of Ge nanostructures formed on the sidewalls of a FIB-fabricated truncated conical structure in Si(001). (a) AFM image, 9.0 × 9.0 $\mu m^2$, from one quadrant of the conical structure, with a depth of 2.3 $\mu$m, on which 7 ML of Ge was deposited. (b) Height $h$ and tilt angle $\theta$ as a function of position along $\varphi = 0$ ([$\bar{1}$10]) from the center of the conical structure toward the rim. (c) Higher resolution AFM image, 3.0 × 3.0 $\mu m^2$, of the region in (a) outlined by the white square ($45 < \varphi < 90°$).

with a regular pitch. Based upon analyses of the results in Figure 1c showing curved nanowires, we fabricate a truncated inverse square pyramid structure in Si having sidewalls with $\theta = 28.2°$ and $\varphi_p = (n90 - 15)°$ ($n = 0, 1, 2, 3$), where we define the azimuthal direction $\varphi_p$ to identify the exposed tilted plane orientations. The base of the pyramidal pit is 15 $\mu$m on a side. This results in four ≃3 × 5 $\mu m^2$ trapezoid-shaped Si{173 100 373} planes, which after flashing and Si buffer growth form a regular corrugated surface morphology as revealed by AFM (not shown). Figure 2a is an AFM image of one of the sidewalls ($\varphi_p = 75°$), corresponding to

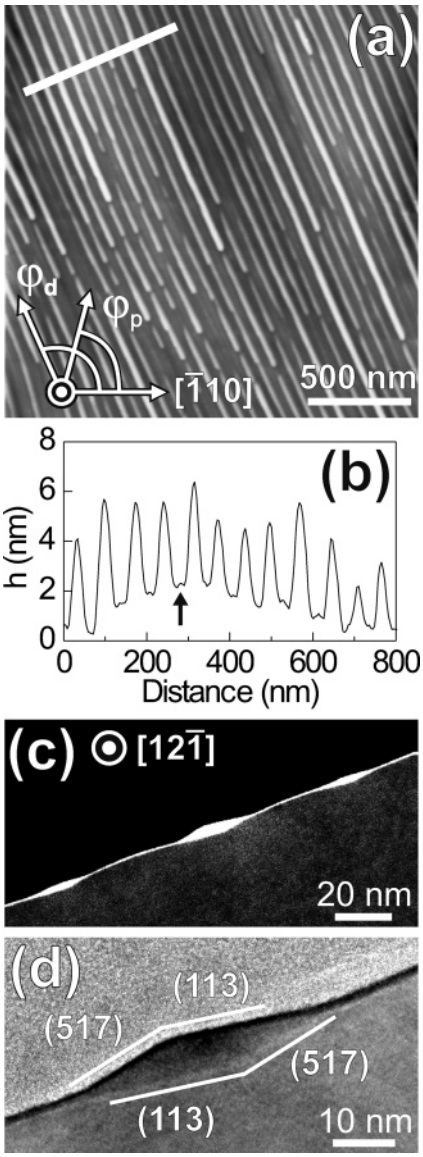


**Figure 2.** Self-organized Ge nanowires formed on Si(173 100 373), corresponding to $\varphi_p = 75°$ with $\theta = 28.2°$. (a) AFM image with a scan size of $2.0 \times 2.0\ \mu m^2$. (b) Height $h$ as a function of position along the white line in (a). (c) Z-contrast STEM image of Ge nanowires shown in (a). (d) High-resolution [12$\bar{1}$] zone-axis XTEM image.

(173 100 373), after depositing 7 ML of Ge. Straight coherent Ge nanowires are formed with lengths extending to several $\mu$m, limited only by the size of the FIB-fabricated structure. The Ge nanowires are aligned along a direction $\varphi_d = 114°$ (i.e., along [72 187 $\overline{84}$]) with respect to [$\bar{1}$10]. Figure 2b, an AFM profile along the white line in Figure 2a, shows that the nanowires are 40 nm wide with a period of 60 nm. The small bumps between two neighboring nanowires, indicated by the arrow in Figure 2b, suggest that Ge nanowires, as demonstrated below, grow along the template grooves on the Si(173 100 373) plane.

Figure 2c is a Z-contrast high-angle annular dark-field STEM image of the Ge nanowires shown in Figure 2a. The micrograph was obtained along the [12$\bar{1}$] zone-axis, which is 5.3° from the nanowire direction [72 187 $\overline{84}$]. The image contrast is due to atomic mass; thus the bright regions correspond to Ge. The interface forms a corrugated hill-and-valley structure composed of two different facet planes. The Ge nanowires, embedded in a thin wetting layer, have a parallelogram-shaped cross-section and reside in valleys formed by the opposing Si facets. The substrate surface structure shown here is analogous to that predicted theoretically by Shchukin[15] for a GaAs(311)*A* surface consisting of a hill-and-valley structure composed of equivalent (3$\bar{1}$3) and (33$\bar{1}$) facets. We determined the facet orientations at the Ge/Si interface based upon high-resolution bright-field XTEM images (see, for example, Figure 2d) to be (113) and (517). Note that (517) is 2.4° off (15 3 23), one of seven major facets observed on well-annealed Ge and Si surfaces.[16] The corresponding facets on the Ge nanowire surface are also (113) and (517). No dislocations were observed in Ge nanowires formed on the Si hill-and-valley template surface.

Next, we consider the general conditions required to obtain a (113)/(517) hill-and-valley template structure at tilt angle $\theta_{HV}$ as a function of $\varphi_p$, i.e., $\theta_{HV}(\varphi_p)$, and use the results to form other types of nanostructures with controlled shapes. The ridgeline of the hill-and-valley structure, which is formed by the intersection of (113) and (517) facets, corresponds to the [12$\bar{1}$] direction. From geometric considerations, any plane obtained by rotating (113) toward (517) around the pivot axis [12$\bar{1}$], which can be expressed as ($k$ 100 200+$k$) with $100 < k < 500$, will form a (113)/(517) hill-and-valley structure with varying ratios $R$ of the widths of (113) to (517) facets. This rotation is equivalent to changing $\theta_{HV}$ from 36.1° with $\varphi_p = 56.3°$ (the (517) plane) to $\theta_{HV} = 25.2°$ with $\varphi_p = 90.0°$ (the (113) plane) with the ridgeline direction of the hill-and-valley structure constant at $\varphi_d = 108.4°$ (i.e., [12$\bar{1}$]). In Figure 1, for example, we observe nanowires within the interval $69° \le \varphi \le 83°$ for which we calculate $\theta_{HV}$ values ranging from 30.1 to 26.3°, which includes the actual tilt angle $\theta = 28.2°$ of the conical structure used in this experiment, and $R$ values from 0.85 to 5.09. This implies a tunable periodicity in hill-and-valley structures composed of (113) and (517) facets, simply by varying $\theta$ and $\varphi$.

These initial results indicate that directed self-assembly of nanostructures with virtually any shape can be achieved by suitable choice of high-index template surfaces. Note that $\varphi_p$ is different for (113) and (517) facets and that neither are equal to $\varphi_p$ for (173 100 373), which is equivalent to $\varphi_p = 75.0°$ with $\theta = 28.2°$. This allows us, through the choice of $\theta$ and $\varphi_p$ during sample preparation by FIB, to change the direction of the intersection lines between the (113)/(517) facets and the exposed growth plane. As a final illustration of this geometric representation for surface nanogroove transformations, we demonstrate results for transforming Ge nanostructures from nanowires to "teardrops".

Figures 3a and 3b are AFM images of Ge nanostructures grown on planes with tilt angles $\theta$ of 24.7 and 31.9°, respectively, and an azimuthal tilt direction $\varphi_p$ of 75°. This corresponds to −3.5 and +3.7° off the (173 100 373) plane toward [173 100 $\overline{107}$]. By decreasing (increasing) $\theta$ slightly from $\theta = 28.2°$ (which results in long straight Ge nanowires), the shape of as-deposited Ge nanostructures is transformed

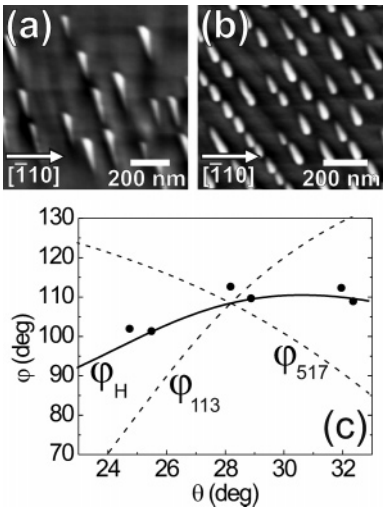


**Figure 3.** Shape transformation from nanowires into "teardrops" resulting from a change in the intersection directions between (113)/(517) facets and the exposed growth planes. AFM images, 1.0 × 1.0 $\mu$m$^2$, of Ge teardrop nanostructures formed on planes with tilt angles (a) $\theta = 24.7$ and (b) 31.9° and an azimuthal direction $\varphi_p$ of 75°. Note that the [1̄10] direction, which corresponds to the scan direction projected onto the (001) plane, is not in the growth planes. (c) Calculated azimuthal directions $\varphi_{113}$ and $\varphi_{517}$ of the intersection lines between (113)/(517) facets and a plane with $\varphi_p = 75°$ as a function of the tilt angle $\theta$. $\varphi_H$ is the azimuthal half-angle between $\varphi_{113}$ and $\varphi_{517}$. Measured $\varphi_H$ values are superimposed as solid circles.

into rows of upward (downward) teardrops with their left (right) sides aligned. In Figure 3a, the azimuthal angles for the left ($\varphi_L$) and right ($\varphi_R$) sides of teardrops are 110.3 and 93.6°, respectively, while $\varphi_L = 97.3°$ and $\varphi_R = 127.4°$ in Figure 3b. This shape transformation follows directly from changes in the intersection directions between the two facets (113)/(517) with the growth plane.

A quantitative description of the shape transformation can be obtained by considering the geometric relationships between the facets and growth planes. The dashed lines in Figure 3c show the calculated azimuthal directions $\varphi_{113}$ and $\varphi_{517}$ of the intersections of (113) and (517) facets with exposed planes at $\varphi_p = 75°$ as a function of $\theta$. The solid line ($\varphi_H$) is the half azimuthal angle, $(\varphi_{113}+\varphi_{517})/2$. As we increase $\theta$ from 24.0 to 32.0°, $\varphi_{113}$ increases from 70.3 to 129.3° while $\varphi_{517}$ decreases from 121.4 to 90.5°, indicating that the intersection directions rotate in opposite directions. $\varphi_{113}$ and $\varphi_{517}$ cross at $\theta = 28.2°$ with $\varphi = 108.4°$, corresponding to the condition in which the tilted growth plane, (173 100 373), has a straight hill-and-valley structure composed of (113) and (517) facets. Measured half azimuthal angles $(\varphi_R+\varphi_L)/2$ of Ge nanostructures plotted in Figure 3c as solid circles exhibit good agreement with the calculated curve $\varphi_H$. This ensures that the basis structure of the growth surface can be formed by (113) and (517) facets over the entire tilt angle range from 24 to 32°.

In summary, we have developed a novel approach, applicable to any materials system, for systematically and rapidly obtaining very-high-index substrate orientations that allow the directed growth of highly-ordered self-organized nanostructures. A surface structural model for the formation of regular nanoscale substrate surface features is used to provide the tilt and azimuthal angles, with respect to the initial substrate surface, required to isolate families of template structures with nanoscale facetting arrays (e.g., hill-and-valley structures), on which desired shape-, size-, and position-controlled nanostructures can be grown. These results are then used as input for computer-controlled FIB fabrication to isolate substrate growth planes. Utilizing this approach, we demonstrate, as an illustration, the formation of Ge nanowires and teardrops, with uniform shape, dimension, and periodicity, on Si(173 100 373) and related surfaces. (173 100 373) is a member of the family of ($k$ 100 200+$k$) planes composed of a (113)/(517) hill-and-valley structure, in which the ratio $R$ of the two facet widths can be controllably varied ($R = 1.7$ for (173 100 373)).

**Acknowledgment.** The authors gratefully acknowledge the financial support of the U.S. Department of Energy (DOE), Division of Materials Science, under Contract No. DEFG02-91ER45439 through the University of Illinois Frederick Seitz Materials Research Laboratory (FS-MRL). We also appreciate the use of facilities in the Center for Microanalysis of Materials, partially supported by DOE, at FS-MRL.

## References

(1) Ito, T.; Okazaki, S. *Nature* **2000**, *406*, 1027−1031.
(2) Mo, Y.-W.; Savage, D. E.; Swartzentruber, B. S.; Lagally, M. G. *Phys. Rev. Lett.* **1990**, *65*, 1020−1023.
(3) Vailionis, A.; Cho, B.; Glass, G.; Desjardins, P.; Cahill, D. G.; Greene, J. E. *Phys. Rev. Lett.* **2000**, *85*, 3672−3675.
(4) Chaparro, S. A.; Zhang, Y.; Drucker, J.; Chandrasekhar, D.; Smith, D. J. *J. Appl. Phys.* **2000**, *87*, 2245−2254.
(5) Capellini, G.; De Seta, M.; Spinella, C.; Evangelisti, F. *Appl. Phys. Lett.* **2003**, *82*, 1772−1774.
(6) Ogino, T.; Homma, Y.; Kobayashi, Y.; Hibino, H.; Prabhakaran, K.; Sumitomo, K.; Omi, H.; Suzuki, S.; Yamashita, T.; Bottomley, D. J.; Ling, F.; Kaneko, A. *Surf. Sci.* **2002**, *514*, 1−9.
(7) Kamins, T. I.; Williams, R. S. *Appl. Phys. Lett.* **1997**, *71*, 1201−1203.
(8) Watanabe, F.; Cahill, D. G.; Hong, S.; Greene, J. E. *Appl. Phys. Lett.* **2004**, *85*, 1238−1240.
(9) Gibson, J. M.; McDonald, M. L.; Unterwald, F. C. *Phys. Rev. Lett.* **1985**, *55*, 1765−1767.
(10) Zhang, X.-J.; Xue, G.; Agarwal, A.; Tsu, R.; Hasan, M.-A.; Greene, J. E.; Rockett, A. *J. Vac. Sci. Technol. A* **1993**, *11*, 2553−2561.
(11) Bramblett, T.; Liu, Q.; Lee, N.-E.; Taylor, N.; Hasan, M.-A.; Greene, J. E. *J. Appl. Phys.* **1995**, *77*, 1504−1513.
(12) Greene, J. E. *MRS Bull.* **2001**, *26*, 777−789.
(13) Cho, B.; Schwarz-Selinger, T.; Ohmori, K.; Cahill, D. G.; Greene, J. E. *Phys. Rev. B* **2002**, *66*, 195407−195411.
(14) Kamins, T. I.; Williams, R. S.; Basile, D. P. *Nanotechnology* **1999**, *10*, 117−121.
(15) Shchukin, V. A.; Borovkov, A. I.; Ledentsov, N. N.; Kop'ev, P. S. *Phys. Rev. B* **1995**, *51*, 17767−17779.
(16) Gai, Z.; Zhao, R. G.; Li, W.; Fujikawa, Y.; Sakurai, T.; Yang, W. S. *Phys. Rev. B* **2001**, *64*, 125201.

NL048340W